# L-band scintillation activity and space-time structure of low-latitude UHF scintillations

A. Bhattacharyya

Indian Institute of Geomagnetism, Mumbai, India

K. M. Groves, S. Basu, and H. Kuenzler

Air Force Research Laboratory, Space Vehicles Directorate, Hanscom Air Force Base, Massachusetts, USA

C. E. Valladares and R. Sheehan

Institute for Scientific Research, Boston College, Chestnut Hill, Massachusetts, USA

[1]   Spatial correlation function of intensity scintillation patterns produced by the propagation of a UHF signal through irregularities in the nighttime low-latitude ionosphere is deduced from an analysis of spaced receiver records of such scintillations. This analysis requires that random temporal variations of the irregularity drift speed be taken into account. It is seen from the results that the occurrence of strong scintillations on an L-band signal requires the presence of short ($\sim$20 m) coherence scale lengths in the UHF scintillation pattern obtained in the plane of the receiver. This condition is satisfied near the crest of the equatorial ionization anomaly (EIA) region, but not near the dip equator. In the decay phase of L-band scintillations recorded near the crest of the EIA region, the maximum strength of these scintillations at any point in time is found to be correlated with the magnetic eastward drift speed of the pattern of intensity scintillations on an UHF signal recorded in this region, which is determined mainly by the magnetic eastward drift velocity of the ionospheric irregularites. Dependence of the corresponding strength of UHF scintillations on the drift speed indicates that toward the end of the decay phase of L-band scintillations, the irregularity power spectrum steepens, and the large scale irregularites that remain can cause the UHF signal to be focused in the plane of the receiver, yielding UHF $S_4$-indices greater than one, while focusing of the UHF signal is less evident at earlier times when there is focusing of the L-band signal.    INDEX TERMS: 2415 Ionosphere: Equatorial ionosphere; 2439 Ionosphere: Ionospheric irregularities; 2487 Ionosphere: Wave propagation (6934); KEYWORDS: equatorial, ionosphere, scintillations

Citation:   Bhattacharyya, A., K. M. Groves, S. Basu, H. Kuenzler, C. E. Valladares, and R. Sheehan, L-band scintillation activity and space-time structure of low-latitude UHF scintillations, Radio Sci., 38(1), 1004, doi:10.1029/2002RS002711, 2003.

## 1.  Introduction

[2]   A number of studies of nighttime ionospheric scintillations near the magnetic equator and in the vicinity of the equatorial anomaly have established that there is a pronounced difference in the levels of L-band scintillations observed in these two regions [Mullen et al., 1985; Groves et al., 1997]. It is well known that plasma depletions or bubbles, in the postsunset equato-

rial ionosphere, tend to become highly structured as they rise from the bottom side of the equatorial F region and penetrate to its topside. This is seen in the plumes captured on radar backscatter maps [Kelley, 1989; Hysell and Kelley, 1997] as well as in theoretical models of nonlinear evolution of the Rayleigh-Taylor instability which gives rise to the plasma bubbles in the equatorial F region [Keskinen et al., 1998]. These bubbles, which are nearly aligned with the geomagnetic field lines, may occasionally rise to altitudes exceeding 800 km, and in the process map down to equatorial ionization anomaly (EIA) regions. Near the crest of the EIA regions, ambient

*F* region ionization density is greater than that near the dip equator, by even as much as a factor of 5. Hence, it has been argued that for a given irregularity amplitude, variation in electron density associated with the plasma bubble irregularities is large enough to produce strong L-band scintillations in the vicinity of EIA regions, while only weak L-band scintillations may be observed near the dip equator. On account of the power law nature of the spectrum of electron density variations in these irregularities, strong VHF/UHF scintillations may be observed near the dip equator as well as EIA regions.

[3] Multifrequency amplitude scintillation data from the EIA region, however, has demonstrated that strong VHF/UHF scintillations in this region are not always accompanied by L-band scintillations [*Basu et al.*, 1983; *Franke and Liu*, 1983, 1985; *Franke et al.*, 1984]. It is well known that in the regime of strong scintillations, the $S_4$-index, which is the standard deviation of normalized intensity variations and is used as a measure of the strength of scintillations, is no longer proportional to irregularity strength as measured by the rms variation in electron density [*Yeh and Liu*, 1982]. In the past, single receiver measurements of VHF, L- and C-band scintillations, at a location near the crest of the EIA, have been used to show that the inverse of the 50% decorrelation time of VHF scintillations may be used to track weak to moderate scintillations on the higher frequencies, since this decorrelation time may be considered to be inversely proportional to the strength of the irregularities, provided the irregularity drift speed and certain characteristics of the power spectrum of the density variations remain unchanged [*Basu et al.*, 1983; *Franke and Liu*, 1985].

[4] In a realistic situation, the speed with which irregularities drift across the signal path is found to be highly variable before 22:00 Hrs local time (LT) [*Bhattacharyya et al.*, 2001] and during the course of a night when scintillations are observed, the drift speed of the ground scintillation pattern often decreases by as much as 50% as seen from results derived using spaced receiver scintillation records [*Valladares et al.*, 1996; *Kil et al.*, 2000]. Random fluctuations in irregularity characteristics, including their drift speeds is, in fact, taken into account in an estimation of the true drift speed of the ground scintillation pattern from spaced receiver scintillation observations [*Vacchione et al.*, 1987; *Spatz et al.*, 1988; *Bhattacharyya et al.*, 1989, 2001]. Ideally, the form of the space-time correlation function for intensity variations should be known, such that the 50% decorrelation scale length, designated the coherence distance $d_I$, of the ground scintillation pattern obtained at any instant of time, may be determined independent of the drift speed of the irregularities or their temporal variability. In this paper, spaced receiver observations of scintillations on a 244 MHz signal at Ascension Island, near the crest of the EIA region, and at Ancon, near the dip equator, are

used to deduce the forms of the space-time correlation functions of intensity scintillations on this signal, and hence the distribution of $d_I$ in the two regions. The results, which are independent of the irregularity drift or its variability, are compared with those derived from a theoretical investigation of the space-time correlation function of intensity scintillations due to a 'deep' random phase screen with a Gaussian spatial correlation function for phase variations in the screen [*Franke*, 1987]. On the basis of these results, it is possible to examine the relationship that the occurrence of strong L-band scintillations and its subsequent decay, has with the form of the space-time correlation function of intensity scintillations on a 244 MHz signal recorded simultaneously with L-band scintillations in the EIA region.

## 2. Space-Time Structure of UHF Signal Intensity

[5] In the analysis, intensity scintillations have been considered instead of amplitude scintillations in order to allow comparison with theoretical results. In the low-latitude region, drift $V_0$ of the ground scintillation pattern, produced by nighttime *F* region irregularities, is usually determined along the magnetic east-west direction using observations made with two receivers spaced along a baseline in this direction. Intensity scintillation data for a 244-MHz signal transmitted from a geostationary satellite and recorded by a set of spaced receivers at each of the two locations: Ascension Island (8.0°S, 14.4°W) which is situated close to the crest of the equatorial anomaly, at a magnetic latitude of about 15°S; and Ancon (11.8°S, 77.2°W, dip latitude 0.9°N) located near the magnetic equator; are used to demonstrate the distinct distribution patterns of $d_I$ in these two regions. For the estimation of $V_0$ from intensity scintillation data using classical correlation analysis techniques, it is assumed that the space-time correlation function of intensity, for variations in one dimension, is of the form [*Briggs*, 1984]:

$$C_I(x, t) = f\left[ (x - V_0 t)^2 + V_C^2 t^2 \right]. \qquad (1)$$

Here $f$ is a monotonically decreasing function of its argument, with $f(0) = 1$, $V_0$ is the average drift speed of the ground scintillation pattern along the baseline, and the parameter $V_C$, generally referred to as the random velocity, is a measure of the decorrelation between the signals recorded by the two receivers, due to random changes in the characteristics of the irregularities. The form of $f$ is not required in the estimation of $V_0$ and $V_C$ from data. However, the coherence scale $d_I$ defined by

$$C_I(x = d_I, t = 0) = 0.5 \qquad (2)$$
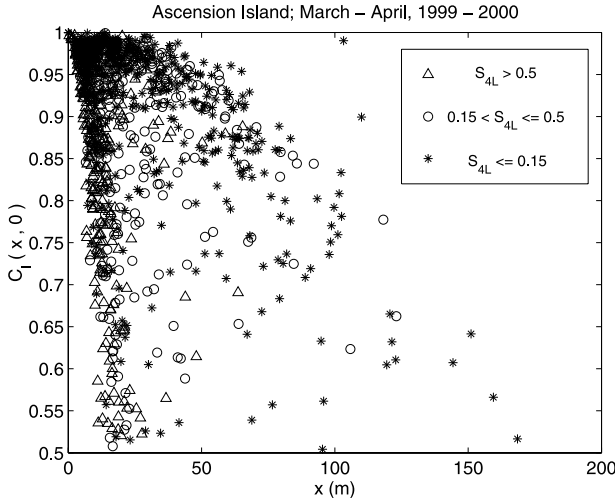
**Figure 1.** Spatial correlation function $C_I(x, 0)$ of intensity scintillation pattern in the plane of the receiver, versus spatial lag $x$, for UHF scintillations recorded at Ascension Island during March–April, 1999 and 2000. The points are assigned different symbols corresponding to different levels of L-band scintillations recorded simultaneously with the UHF scintillations.

depends on the form of the function $f$. From (1), given that $f$ is a monotonically decreasing function of its argument, it is seen that for two receivers separated by a fixed distance $x_0$, the maximum cross-correlation $C_I(x_0, t_m)$ occurs at a time lag $t_m$ for which the argument of the function $f$ is a minimum. This yields

$$t_m = \frac{x_0 V_0}{V_0^2 + V_C^2} \quad (3)$$

and

$$C_I(x_0, t_m) = f\left[\frac{x_0^2 V_C^2}{V_0^2 + V_C^2}\right] \quad (4)$$

According to (4), consideration of $C_I(x_0, t_m)$ as a function of $x_0^2 V_C^2/(V_0^2 + V_C^2)$ reveals the form of $f$. In particular, the spatial correlation function, $C_I(x, 0)$, of the ground scintillation pattern along the baseline of the receivers, at any instant of time, may be obtained as a function of spatial lag $x$ by simply plotting $C_I(x_0, t_m)$ versus $x_0 V_C/(V_0^2 + V_C^2)^{1/2}$. The required values of $C_I(x_0, t_m)$, $V_0$, and $V_C$ are estimated from spaced receiver scintillation observations. The data used in the present analysis consist of the intensity of the signal recorded at intervals of .02s during the course of a scintillation event. Auto- and cross-correlation functions of the two signals are evaluated for approximately 82s intervals using 4096 data points at a time. Irregularity characteristics continue to change throughout the course of a scintillation event.

Hence for a given event, $C_I(x, 0)$ also evolves, yielding different coherence scales $d_I$, as the scintillation event unfolds. Since the evolution of the irregularities depends on the location and season, mass plots of $C_I(x, 0)$ versus $x$, derived from spaced receiver scintillation data recorded at a particular location, are restricted to a particular time of the year. Such a mass plot for Ascension Island using data of 9 nights in March–April 1999, and of 12 nights in March–April 2000, is shown in Figure 1. Mass plot of $C_I(x, 0)$ as a function of $x$ for Ancon, during February–March, 1999, is displayed in Figure 2, while Figure 3 depicts such a mass plot for Ancon during October 1999.

## 3. L-Band Scintillations and $C_I(x, 0)$

[6] As stated in the introduction, it is well known that the occurrence statistics of L-band scintillations are vastly different near the magnetic equator and near the crest of the EIA region. *Groves et al.* [1997] used data from the equatorial station Huancayo, for the period 1986–1989, to establish that fading depths as low as 2 dB are encountered there for only 20% of the time, even during the solar maximum period when L-band scintillation occurrence reaches its peak. Therefore, the L-band $S_4$-index does not generally exceed 0.2 at an equatorial location. In contrast, strong L-band scintillations are recorded at Ascension Island near the EIA crest, in the time interval of 20–24 LT, during the months of September to April, around sunspot maximum [*Aarons*, 1993; *Groves et al.*, 1997]. The top and bottom panels of
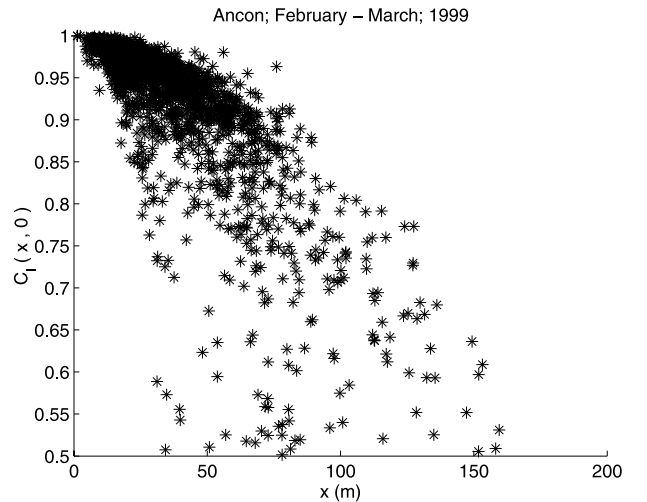


**Figure 2.** Spatial correlation function $C_I(x, 0)$ of intensity scintillation pattern in the plane of the receiver, versus spatial lag $x$, for UHF scintillations recorded at Ancon during February–March, 1999.
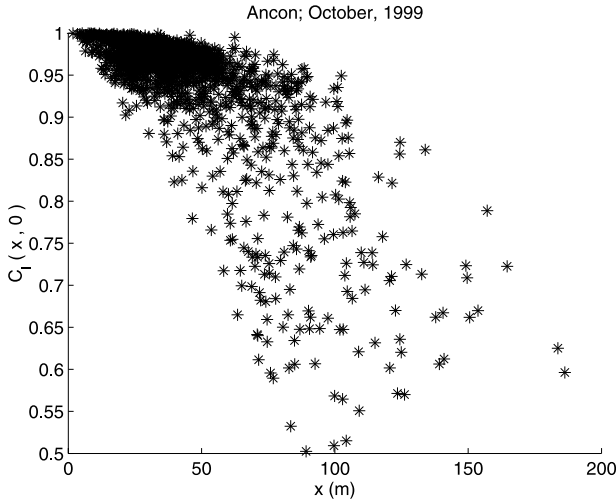
**Figure 3.** Spatial correlation function $C_I$ $(x, 0)$ of intensity scintillation pattern in the plane of the receiver, versus spatial lag $x$, for UHF scintillations recorded at Ancon during October, 1999.

Figure 4 display the distribution of Ascension Island L-band $S_4$-indices as a function of local time for 9 nights of March−April 1999, and 12 nights of March−April 2000, respectively. The average sunspot numbers for these sets of days are 72 and 163 respectively. With increasing solar activity, the local time interval for occurrence of L band scintillations at Ascension Island is extended.

[7] A comparison of the distribution of L-band and 244 MHz scintillations recorded at Ascension Island during March−April, 2000 is presented in Figure 5. As noted in the introduction, there is no direct relationship between the strength of scintillations on 244 MHz, and the strength of L-band scintillations as represented by the respective $S_4$-indices. However, one feature to be noted in Figure 5 is the greater tendency of the 244 MHz $S_4$-index to exceed 1 as the L-band scintillations decay. Going back to Figure 1, which is also a mass plot of $C_I(x_0, t_m)$ as a function of $x_0 V_C / (V_0^2 + V_C^2)^{1/2}$ for Ascension Island, each point is labeled by the corresponding value of L-band $S_4$-index ($S_{4L}$). For this purpose, values of $S_{4L}$ have been divided into three categories: weak ($S_{4L} \leq 0.15$), moderate ($0.15 < S_{4L} \leq 0.5$), and strong ($S_{4L} > 0.5$), and each category has been represented by a different symbol. Thus Figure 1 also depicts the distribution of the points according to the strength of L-band scintillations. Before discussing this aspect of Figure 1, it is noted that the 244-MHz and L-Band (1.612 GHz) signals are transmitted from two different geostationary satellites. The subionospheric point for the 244-MHz signal is located 20 km to the east of the subionospheric point for the L-band signal. Hence, $S_{4L}$ values obtained from the data do not
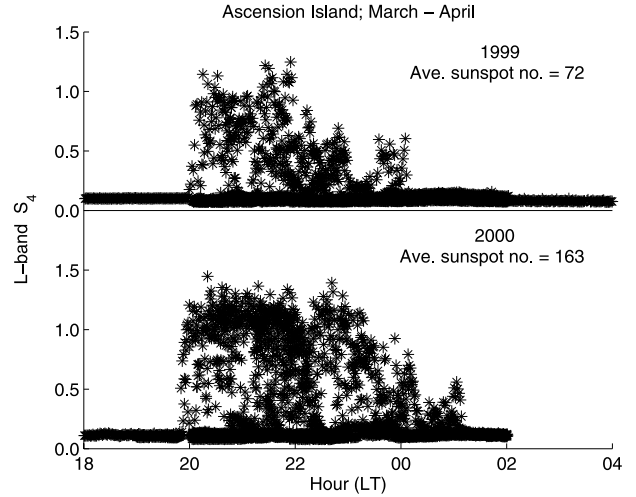


**Figure 4.** Distribution of L-band $S_4$-indices obtained at Ascension Island, as a function of local time, for 9 nights of March−April, 1999 (top panel) and 12 nights of March−April, 2000 (bottom panel). The average values of sunspot numbers for the two periods are given in the figure.

correspond exactly to the points plotted in Figure 1, but most of the points associated with strong L-band scintillations are seen from Figure 1 to correspond to the smallest values of the coherence scale $d_I$, while the weakest L-band scintillations generally tend to be associated with those points which correspond to the largest values of $d_I$. The conclusion that may be drawn
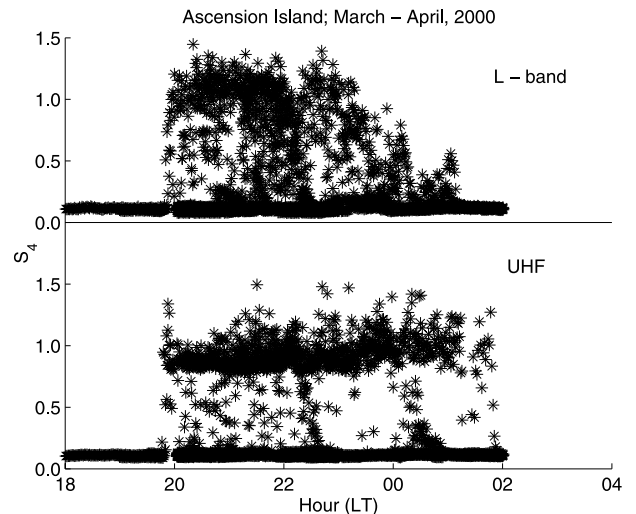


**Figure 5.** Comparison of the distributions of L-band (top panel) and UHF (bottom panel) $S_4$-indices obtained at Ascension Island, as a function of local time, during March−April, 2000.

from Figure 1 is that strong scintillations would occur on an L-band signal whenever the coherence scale length of the 244 MHz scintillation pattern falls below 30m. It is seen from Figures 2 and 3, that this condition is not satisfied by the coherence scale lengths of the 244 MHz intensity scintillation patterns obtained at Ancon either in February–March, 1999, or in October, 1999. This explains the absence of strong L-band scintillation observations at Ancon. By studying the auto-correlation function of 257-MHz scintillations recorded by a single receiver at Ascension Island, *Basu et al.* [1983] had found the inverse of the 50% decorrelation interval to be a good measure of the strength of irregularities whenever the drift speed of the ground scintillation pattern did not vary significantly. *Franke and Liu* [1985] provided a theoretical explanation for this observation.

## 4. Comparison With Theory

[8] In the limiting case where intensity scintillations produced by a phase-changing screen are considered to be saturated, statistics of the intensity field below the phase screen converge to a Gaussian limit. Under such conditions, space-time covariance function for variations in the normalized intensity, $I(x, t)$, of the ground scintillation pattern is simply related to the phase structure function of the phase screen [*Yeh and Liu*, 1982]. This relationship takes the form:

$$B_I(x,t) = \langle I(x+x', t+t')I(x',t')\rangle = 1 + \exp\left[-D_\phi(x,t)\right]$$
(5)

where $D_\phi(x, t)$ is the structure function for phase variations in the phase screen:

$$D_\phi(x,t) = \langle[\phi(x+x', t+t') - \phi(x',t')]^2\rangle$$
(6)

The angular brackets in (5) and (6) denote ensemble averaging. For a situation where the motion of the irregularities may be considered as 'frozen', such that they simply convect with a uniform velocity, without any temporal changes, and with the assumption that the coherence scale of the intensity pattern is much smaller than a characteristic scale length associated with the irregularity spectrum, it has been shown that the inverse of the 50% decorrelation interval for intensity scintillations, $\tau_I$, is proportional to the standard deviation, $\sigma_\phi$, of phase variations in the phase screen [*Franke and Liu*, 1985]. For a two-component power law spectrum of density variations in the irregularities, the characteristic scale length is the 'break scale', whereas for a single component power law spectrum, it would be the outer scale. *Franke and Liu* [1985] thus provided a theoretical explanation for the observation that when VHF scintillations were in the saturated regime, the corresponding C-band scintillations, which were weak, yielded an

$S_4$-index proportional to $\sigma_\phi$ and hence to $(1/\tau_I)$, provided the drift velocity of the irregularities, the outer scale, and 'break scale' remained constant.

[9] In the analysis reported in the present paper, allowance has been made for random temporal variations in the irregularities while they drift with an average speed. Hence the results must be compared with a theoretical space-time correlation function for intensity scintillations derived for such a situation. The phase screen approximation has been used to obtain the space-time correlation function for intensity scintillations produced by a 'shallow' screen [*Wernik et al.*, 1983] and a 'deep' screen [*Franke*, 1987], where the models for the statistics of phase fluctuations in the screens allowed random temporal variations in the irregularities' characteristics. Here the qualification of the phase screen as 'shallow' or 'deep' depends on whether changes in optical path length introduced by the screen are smaller or larger than a wavelength of the incident radio wave. As noted by *Franke* [1987], if the irregularities are described by a power law type of spatial spectrum, instead of a Gaussian correlation function which is determined by a single scale length, it is necessary to consider the change in path length produced by irregularities of scale size near the Fresnel scale. One basic question underlying the use of the classical correlation analysis technique [*Briggs*, 1984], to estimate $V_0$ and $V_C$ from spaced receiver scintillation data, concerns the validity of the assumed form of the space-time correlation function given in equation (1). For weak intensity scintillations on a signal, which has propagated through a 'shallow' phase screen, theoretical calculations have shown that this assumption is valid [*Wernik et al.*, 1983]. The other extreme situation that has been considered, is that of saturated scintillations produced by a one-dimensional 'deep' phase screen, with a Gaussian spatial correlation function characterized by a length scale $l_0$. In this case, allowing the irregularities which constitute the phase screen to have a Gaussian velocity distribution with mean $V_0$ and variance $\sigma_V^2$, *Franke* [1987] showed that for time lags $t \ll l_0/\sigma_V$, the space-time covariance function for intensity scintillations may be obtained from:

$$B_I(x,t) = 1 + \exp\left\{-\frac{2\sigma_\phi^2}{l_0^2}\left[(x - V_0 t)^2 + \sigma_V^2 t^2\right]\right\}$$
(7)

and thus the space-time correlation function of intensity scintillations assumes the form

$$C_I(x,t) = \frac{B_I(x,t) - 1}{B_I(0,0) - 1} = \exp\left\{-\frac{2\sigma_\phi^2}{l_0^2}[(x - V_0 t)^2 + \sigma_V^2 t^2]\right\}$$
(8)

This satisfies the assumption inherent in (1) with the identification of $V_C$ with $\sigma_V$.

[10] From Figure 1 it appears that the ground scintillation patterns at Ascension Island, near the crest of the EIA, tend to fall into two broad categories: one with coherence scale lengths centered around $d_I \simeq 20$ m and the other with $d_I \geq 150$ m. On the other hand, at Ancon near the dip equator, coherence scale lengths seem to be evenly distributed between approximately 40 m and 160 m during the scintillation events of February–March, 1999, as depicted in Figure 2. The same is true of scintillation events recorded at Ancon during October 1999, except that the lower and upper limits for $d_I$ are approximately 70 m and 200 m, which are much larger than those found for February–March 1999. Numerical modeling is required to understand this seasonal difference in the distribution of $d_I$ seen in the scintillation patterns at Ancon for these two periods. In the present paper, the aim is to understand the relationship between occurrence of strong L-band scintillations and space-time structure of UHF scintillations. Hence, (8) is used for a comparison with results derived from data. According to (8), the spatial correlation function for intensity variations, $C_I(x, 0)$, has a Gaussian form:

$$C_I(x, 0) = \exp\left[-\frac{2\sigma_\phi^2}{l_0^2}x^2\right] \qquad (9)$$

For comparison with $C_I(x, 0)$ derived from data, two theoretical curves are drawn in Figure 6, using (9) with two different values of $b = 2\sigma_\phi^2/l_0^2$. It is seen that there is an order of magnitude difference between the values of $\sigma_\phi/l_0$ for the two predominant groups of $C_I(x, 0)$ estimated from Ascension Island UHF scintillation data.
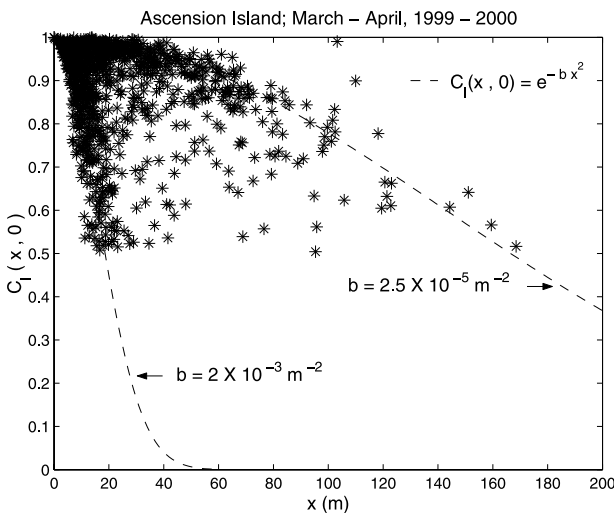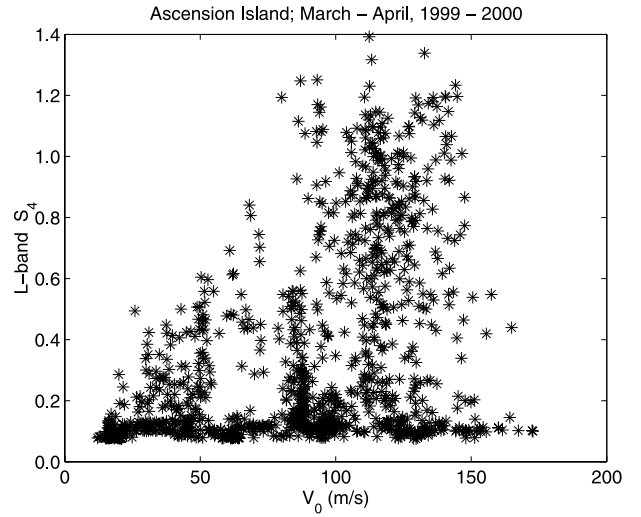


**Figure 7.** Variation of L-band $S_4$-indices with the magnetic eastward drift, $V_0$, of the UHF ground scintillation pattern obtained at Ascension Island during March–April, 1999 and 2000.

From this it can be concluded that, as expected, occurrence of L-band scintillations requires the presence of small scale length irregularities, corresponding to small values of $l_0$, and of large density variations which would yield a large $\sigma_\phi$. From this simple picture, it is not possible to delineate the roles of $\sigma_\phi$ and $l_0$ separately in producing strong L-band scintillations. However, (9) is seen to provide a reasonable description of the spatial correlation functions of UHF intensity scintillation patterns with small coherence scale lengths $d_I$.

## 5. L-Band Scintillations and $V_0$

[11] In the previous section, low-latitude ionospheric irregularities are described in terms of a phase-changing screen, and the irregularity characteristics, that are required for producing strong L-band scintillations, are extracted from spaced receiver intensity scintillation data on a UHF signal. In this section, it is investigated whether the spaced receiver data can shed some light on the decay of L-band scintillations. A plot of L-band $S_4$ versus $V_0$, the magnetic eastward drift of the ground scintillation pattern for the UHF signal recorded at Ascension Island during March–April of years 1999 and 2000, is displayed in Figure 7. This figure shows that in the decay phase of L-band scintillations, maximum possible value of L-band $S_4$ appears to be correlated with $V_0$. Smaller the value of $V_0$, smaller is the maximum strength of scintillations that might be observed on an L-band signal. A plot of UHF $S_4$ versus $V_0$ (Figure 8), obtained at Ascension Island during March–April, 1999, reveals



**Figure 6.** Comparison of $C_I(x, 0)$ as a function of spatial lag $x$, computed from Ascension Island data, and from theory using two different values of $b = 2\sigma_\phi^2/l_0^2$.
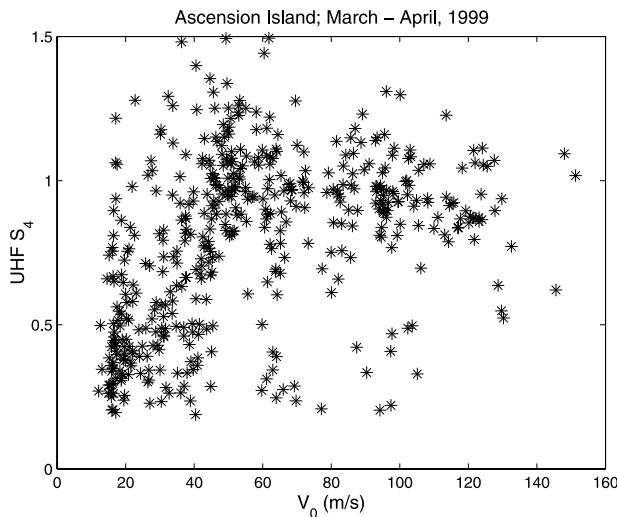
**Figure 8.** Variation of UHF $S_4$-indices with the magnetic eastward drift, $V_0$, of the ground scintillation pattern obtained at Ascension Island during March–April, 1999.

an interesting feature. As $V_0$ falls below 80 m/s, and L-band scintillations start decaying as seen in Figure 7, there is a tendency of the UHF $S_4$ to have values exceeding unity initially as $V_0$ decreases, before the UHF $S_4$ shows a sharp decline. In contrast, for values of $V_0$ above 80 m/s, as $V_0$ increases, the corresponding UHF $S_4$-indices tend to a value of 1. An interpretation of this behavior of the UHF $S_4$-index with changing $V_0$, must be compatible with the results shown in Figure 7. Such an interpretation is that as the value of $V_0$ decreases below about 80 m/s, there is an increasing decay of small scale-length irregularities which cause L-band scintillations, but the larger scale length irregularities remain intact. These large scale length irregularities are able to focus the incident 244 MHz radio waves, yielding UHF $S_4$ values greater than 1. In contrast, when small scale irregularities have a large presence, for values of $V_0$ in excess of 80 m/s, the incident UHF radio wave is scattered by the small scale irregularities, yielding values of UHF $S_4$ that approach unity. These contrasting pictures of focusing and scattering of UHF radio waves in the absence and presence, respectively, of small scale irregularities that are involved in producing L-band scintillations, is in agreement with the theoretical results derived by *Singleton* [1970]. Further, in accordance with *Singleton*'s [1970] result, when sufficiently small scale irregularities have a strong enough presence to scatter UHF radio waves, these irregularities may still have scale sizes large enough to cause focusing of L-band radio signals. This is clearly seen in Figure 7, where L-band $S_4$

values greater than 1 are also encountered for $V_0 > 80$ m/s. Finally, for further decrease in $V_0$ below 40m/s, the large scale irregularities also decay, and the UHF $S_4$-index also decreases rapidly.

## 6. Summary

[12] In this paper the spatial characteristics of the ground scintillation pattern, produced by the propagation of UHF radio waves through nighttime irregularities in the low-latitude ionosphere, are studied using spaced receiver intensity scintillation data recorded for a 244 MHz signal transmitted from a geostationary satellite. In the past such data have been utilized to estimate the zonal drift speed of ionospheric irregularities, and also the parameter $V_C$, which is a measure of random temporal variations in the characteristics of the irregularities. An estimate of the drift speed is also required if information about the spatial scale sizes present in the ground scintillation pattern is to be extracted from power spectra of the recorded scintillations. Contribution of random temporal variations is not taken into account in such calculations. In the present paper, a simple method has been proposed to determine the general forms of a function describing the space-time correlations of scintillation patterns produced on the ground under different scattering conditions, from spaced receiver scintillation records. Once this functional form is established, it directly yields the spatial correlation function of intensity variations in the plane of the receiver at any instant of time. A phase-screen based theory [*Franke*, 1987] is used to relate the UHF intensity correlation function derived from data with the spatial correlation function of ionospheric irregularities which produce the scintillations. This procedure shows that ionospheric irregularities, which have the necessary characteristics for producing strong L-band scintillations, evolve near the crest of the EIA region, during the premidnight period. It is also seen that nighttime $F$ region irregularities near the dip equator, do not have the necessary characteristics, both in terms of scale size and density variation, for producing L-band scintillations. Further, distinct seasonal changes are seen in the spatial characteristics of nighttime UHF scintillations recorded in the equatorial region, which indicate seasonal changes in the spatial structure of corresponding ionospheric irregularities. An understanding of this behavior requires a theoretical calculation of spatial correlation function of intensity scintillations produced by a thick layer of irregularities with a power law spectrum. Preliminary results from such calculations, which shall be reported elsewhere, indicate that the conclusions based on a phase screen model are not invalidated by the numerical results.

[13] It is noted that because the signal path is not vertical, the estimated $V_0$ has contributions from the

magnetic eastward component, $V_E$, as well as the vertical component $V_Z$ of the irregularity drift velocity: $V_0 = V_E - V_Z \tan \theta \sin \lambda$, where $\theta$ is the zenith angle and $\lambda$ is the azimuth of the signal path measured eastward from the north. During the decay phase of L-band scintillations, irregularities drift with a velocity close to that of the ambient plasma [*Bhattacharyya et al.*, 2001] and the contribution of $V_Z$ to $V_0$ may be neglected in comparison to that of $V_E$. As $V_E$ tends to decrease in magnitude throughout the period after approximately 22 LT, during which $S_{4L}$ decreases, the estimated values of $V_0$ at any time during the decay phase of L-band scintillations show a correlation with the maximum value of $S_{4L}$ that may be observed at that time. Thus the decrease in $V_0$ may be treated as a proxy for time elapsed during the decay phase of L-band scintillations. This explains the appearance of focusing effects in UHF scintillations recorded near the crest of the EIA region, only when the estimated $V_0$ decreases from about 140 m/s in the early evening hours to between 40 and 60 m/s in the postmidnight period. For values of $V_0$ above 80 m/s, on the other hand, focusing occurs on L-band but is not pronounced on UHF. Phase screen simulation studies [*Franke and Liu*, 1983] have established that focusing on L-band can only be recoinciled with coherence scales found in VHF scintillation patterns when the irregularities have a two-componenet power law spectrum and that such a spectrum does not produce focusing on a VHF signal. Plasma density data from the AE-E satellite offering a 'horizontal cut' through equatorial $F$ region irregularities in the South American Magnetic Anomaly region around local midnight, have shown that in the decay phase of the irregularities, a two-component power law spectrum is maintained for some time [*Hysell and Kelley*, 1997]. Occurrence of focusing on the UHF signal seen here in the postmidnight hours, when $V_0$ is much reduced, may thus be attributed to a steepening of the spectrum at a later time.

# References

Aarons, J., The longitudinal morphology of equatorial F-layer irregularities relevant to their occurrence, *Space Sci. Rev.*, *63*, 209–243, 1993.

Basu, S., et al., High resolution topside data of electron densities and VHF/GHz scintillations in the equatorial region, *J. Geophys. Res.*, *88*, 403–415, 1983.

Bhattacharyya, A., S. J. Franke, and K. C. Yeh, Characteristic velocity of equatorial $F$ region irregularities determined from spaced receiver scintillation data, *J. Geophys. Res.*, *94*, 11,959–11,969, 1989.

Bhattacharyya, A., et al., Dynamics of equatorial F region irregularities from spaced receiver scintillation observations, *Geophys. Res. Lett.*, *28*, 119–122, 2001.

Briggs, B. H., The analysis of spaced sensor records by correlation techniques, in *Middle Atmosphere Program, Handbook for MAP*, vol. 13, edited by R. A. Vincent, pp. 166–186, Sci. Comm. on Sol.-Terr. Phys., Int. Counc. of Sci. Unions, Paris, 1984.

Franke, S. J., The space-time intensity correlation function of scintillation due to a deep random phase screen, *Radio Sci.*, *22*, 643–654, 1987.

Franke, S. J., and C. H. Liu, Observations and modeling of multifrequency VHF and GHz scintillations in the equatorial region, *J. Geophys. Res.*, *88*, 7075–7085, 1983.

Franke, S. J., and C. H. Liu, Modeling of equatorial multifrequency scintillation, *Radio Sci.*, *20*, 403–415, 1985.

Franke, S. J., C. H. Liu, and D. J. Fang, Multifrequency study of ionospheric scintillation at Ascension Island, *Radio Sci.*, *19*, 695–706, 1984.

Groves, K. M., et al., Equatorial scintillation and systems support, *Radio Sci.*, *32*, 2047–2064, 1997.

Hysell, D. L., Imaging coherent backscatter radar studies of equatorial spread F, *J. Atmos. Sol. Terr. Phys.*, *61*, 701–716, 1999.

Hysell, D. L., and M. C. Kelley, Decaying equatorial $F$ region plasma depletions, *J. Geophys. Res.*, *102*, 20,007–20,017, 1997.

Kelley, M. C., *The Earth's Ionosphere*, *Int. Geophys. Ser.*, vol. 43, pp. 113–120, Academic, San Diego, Calif., 1989.

Keskinen, M. J., S. L. Ossakow, S. Basu, and P. J. Sultan, Magnetic-flux-tube-integrated evolution of equatorial ionospheric plasma bubbles, *J. Geophys. Res.*, *103*, 3957–3967, 1998.

Kil, H., et al., Glabal positioning system measurements of the ionospheric zonal apparent velocity at Cachoeira Paulista in Brazil, *J. Geophys. Res.*, *105*, 5317–5327, 2000.

Mullen, J. P., E. Mackenzie, S. Basu, and H. Whitney, UHF/GHz scintillation observed at Ascension Island from 1980 through 1982, *Radio Sci.*, *20*, 357–365, 1985.

Singleton, D. G., Saturation and focusing effects in radio-star and satellite scintillations, *J. Atmos. Terr. Phys.*, *32*, 187–208, 1970.

Spatz, D. E., S. J. Franke, and K. C. Yeh, Analysis and interpretation of spaced receiver scintillation data recorded at an equatorial station, *Radio Sci.*, *23*, 347–361, 1988.

Vacchione, J. D., S. J. Franke, and K. C. Yeh, A new analysis technique for estimating zonal irregularity drifts and variability in the equatorial $F$ region using spaced receiver scintillation data, *Radio Sci.*, *22*, 745–756, 1987.

Valladares, C. E., et al., The multi-instrumented studies of equatorial thermosphere aeronomy scintillation system: Climatology of zonal drifts, *J. Geophys. Res.*, *101*, 26,839–26,850, 1996.

Wernik, A. W., C. H. Liu, and K. C. Yeh, Modeling of spaced-receiver scintillation measurements, *Radio Sci.*, *18*, 743–763, 1983.

Yeh, K. C., and C. H. Liu, Radio-wave scintillations in the ionosphere, *Proc. IEEE*, *70*, 324–360, 1982.

———————

S. Basu, K. M. Groves, and H. Kuenzler, Air Force Research Laboratory, Space Vehicles Directorate (AFRL/VSBI), 29 Randolph Road, Hanscom AFB, MA 01731-3010, USA. (Santimay.Basu@hanscom.af.mil; Keith.Groves@hanscom.af.mil; Howard.Kuenzler@hanscom.af.mil)

A. Bhattacharyya, Indian Institute of Geomagnetism, Colaba, 400005 Mumbai, India. (archana@iig.iigm.res.in)

R. Sheehan and C. E. Valladares, Institute for Scientific Research, Boston College, Chestnut Hill, MA 02467, USA. (sheehan@plh.af.mil; ceasar@dl5000.bc.edu)